INVESTIGATION OF DIFFERENT LOW-COST LAND VEHICLE NAVIGATION SYSTEMS BASED ON CPD SENSORS AND VEHICLE INFORMATION

M. Moussa [1], A. Moussa [1,2], M. Elhabiby[3], N. El-Sheimy [1]
(mohamed.moussa1@ucalgary.ca, amelsaye@ucalgary.ca, mmelhabi@ucalgary.ca, elsheimy@ucalgary.ca)

[1] Department of Geomatics Engineering, University of Calgary, Calgary, Alberta, Canada
[2] Department of Electrical Engineering, Port-Said University, Port Said, Egypt
[3] Public Works Department, Ain-Shams University, Cairo, Egypt

Commission I, WG I/6

KEY WORDS: Inertial Navigation Systems, Consumer Portable Devices, Steering angle, Dead Reckoning, Reduced Inertial Sensor System, Extended Kalman Filter.

ABSTRACT:

Recently, many companies and research centres have been working on research and development of navigation technologies for self-driving cars. Many navigation technologies were developed based on the fusion of various sensors. However, most of these techniques used expensive sensors and consequently increase the overall cost of such cars. Therefore, low-cost sensors are now a rich research topic in land vehicle navigation. Consumer Portable Devices (CPDs) such as smartphones and tablets are being widely used and contain many sensors (e.g. cameras, barometers, magnetometers, accelerometers, gyroscopes, and GNSS receivers) that can be used in the land vehicle navigation applications.
This paper investigates various land vehicle navigation systems based on low-cost self-contained inertial sensors in CPD, vehicle information and on-board sensors with a focus on GNSS denied environment. Vehicle motion information such as forward speed is acquired from On-Board Diagnosis II (OBD-II) while the land vehicle heading change is estimated using CPD attached to the steering wheel. Additionally, a low-cost on-board GNSS/inertial integrated system is also employed. The paper investigates many navigation schemes such as different Dead Reckoning (DR) systems, Reduced Inertial Sensor System (RISS) based systems, and aided loosely coupled GNSS/inertial integrated system.
An experimental road test is performed, and different simulated GNSS signal outages were applied to the data. The results show that the modified RISS system based on OBD-II velocity, onboard gyroscopes, accelerometers, and CPD-based heading change provides a better navigation estimation than the typical RISS system for 90s GNSS signal outage. On the other hand, typical inertial aided with CPD heading change, OBD-II velocity updates, and Non-Holonomic Constraint (NHC) provide the best navigation result.

1. INTRODUCTION

Global Navigation Satellite System (GNSS) is the most commonly used navigation component in land vehicles where it provides a long-term accurate estimate for position and velocity states (Aggarwal et al., 2008). Unfortunately, GNSS signals suffer from blockage and multipath (Bancroft, 2009) in some operating conditions such as urban areas (Venkatraman et al., 2010) and foliage regions where the navigation solution is blocked or deteriorated.
Inertial Navigation System (INS) provides reliable short-term full navigation estimates (position, velocity, and attitudes) for land vehicles (Iqbal et al., 2010). However, the navigation solution is degraded after a short time due to the INS drift especially for Micro-Electro-Mechanical Systems (MEMS) based INS because of its accelerometers and gyroscopes large errors and noise characteristics (Abd Rabbou and El-Rabbany, 2015).
Therefore, GNSS and INS are integrated to overcome the shortcomings of each sensor and to provide a more reliable navigation solution in both short and long-term periods (Niu et al., 2007).
GNSS/INS has a defect when GNSS signal is blocked for a long time where INS standalone navigation solution will deteriorate quickly due to INS drift. Therefore, INS should be aided with other sensors to mitigate its large drift and to provide a better navigation estimation.
Many aiding sensors are used for land vehicle navigation such as odometers, ultrasonic sensors (M Moussa et al., 2019)(Moussa et al., 2018), magnetometers (Won et al., 2015), Light Detection And Ranging (LIDAR) (Gao et al., 2015)(Tang et al., 2015), cameras (Zhenbo Liu, 2019)(Liu, et al., 2018), and Radio Detection And Ranging (RADAR) (Bo et al., 2018).
Unfortunately, there are many drawbacks for using these sensors such as the magnetic interference in the case of magnetometers, the high price, high computational and processing cost, and the environmental effects in the case of LiDAR and cameras. Finally, sensor installment is a very hard process for the ultrasonic. Maps aiding navigation is used in many previous researches to help low-cost INS in GNSS denied environments (Attia, 2013). Such map aiding depends on the availability and update rate of the required maps.
Consumer Portable Devices (CPDs) are widely used all over the globe. CPDs contain many sensors such as GNSS receivers, low-cost INS, magnetometer, barometer, and camera that can be used in many land vehicles applications such as navigation, lane localization (Song et al., 2017) (Zhu et al., 2017), environmental perception, safety driving monitoring, insurance telematics (Wahlström et al., 2017), and road surface condition monitoring (Sathe and Deshmukh, 2017).
RISS is a Dead Reckoning (DR) navigation system which is categorized into 2D and 3D RISS where 2D RISS consists of one gyroscope and a source of land vehicle forward velocity such as odometer. On the other hand, 3D RISS consists of one gyroscope and two-axis accelerometers along with an odometer (Noureldin et al., 2013). RISS has been addressed in many previous researches, (Iqbal et al., 2008) described the mechanization of RISS as well as its integration with GNSS

through Kalman Filter (KF). 3D RISS/GNSS integrated system through Particle Filter (PF) was addressed in (Georgy et al., 2010a). (Georgy et al., 2010b) integrated RISS along with GNSS through a tightly coupled fusion scheme with PF and compared the results with KF.

Some researchers worked on enhancing the RISS in GNSS denied environment fusing other sensors such as magnetometers to offer a heading update to aid RISS during GNSS signal outage through EKF (Abosekeen et al., 2019).

CAN (Controller Area Network) bus provides some useful information about the vehicle dynamics such as the forward velocity and steering angle data. However, the commercial On-Board Diagnostics (OBD-II) provides the velocity information and does not typically provide the steering angle data unless additional customized hardware and software designs are developed (Xiao et al., 2018).

Therefore, a new method for estimating the steering angle was proposed by (Moussa et al., 2019) through CPD accelerometers and then the land vehicle change of heading is estimated.

The main objective of this paper is to investigate different low-cost land vehicle navigation systems based on CPD sensors and land vehicle information. These navigation systems are based on DR, RISS, and loosely coupled INS/GNSS integrated systems. The outcome of this paper will not only help land vehicle navigation applications but will also open the door for many mobile mapping applications based on CPD sensors.

2. METHODOLOGY

The methodology consists of five subsections: land vehicle heading change estimation using CPD accelerometers, DR navigation system based on heading change estimated by CPD accelerometers and OBD-II velocity, DR navigation system with gyroscope updates, 3D RISS, and typical loosely coupled GNSS/INS with CPD heading change and OBD-II velocity updates during GNSS signal outage.

2.1 CPD accelerometers Heading Change Estimation

Land vehicle heading change estimation using CPD accelerometers is described in details in (Moussa et al., 2019). CPD is mounted on the vehicle steering wheel to estimate the steering angle through CPD accelerometers as shown in Figure 1.

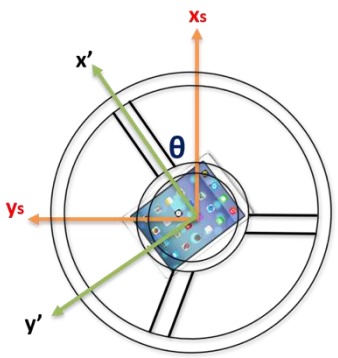

Figure 1. CPD accelerometers axes and the steering wheel fixed axis Car.

The steering angle computation should be compensated for the leveling of the onboard INS, the steering wheel inclination, the vehicle acceleration, and the vehicle inclination. However, all these factors may be ignored if only one CPD is used in the navigation state estimation, i.e. when no onboard INS is used. Therefore, the steering wheel angle is estimated as shown in equation 1.

$$\tan\theta = \frac{a_{y'}}{a_{x'}} \tag{1}$$

Where $a_{y'}$ and $a_{x'}$ are the CPD accelerometers of y and x-axis, θ is the steering wheel angle.

If there is an onboard INS, all the factors are compensated from the CPD steering wheel angle estimation as shown in Figure 2, and equation 2 (Moussa et al., 2019).

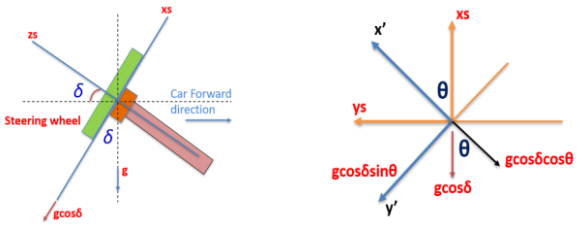

Figure 2. Steering wheel angle and steering inclination angle

$$\tan\theta = \frac{-a_{x'}a_{Y_v'} - a_{y'}[a_{X_v'}\sin\delta - g\cos\delta - a_{Z_v'}\cos\delta]}{a_{x'}[a_{X_v'}\sin\delta - g\cos\delta - a_{Z_v'}\cos\delta] - a_{y'}a_{Y_v'}} \tag{2}$$

Where δ is the steering wheel inclination angle, g is the gravity acceleration, $a_{xv'}$, $a_{yv'}$, *and* $a_{zv'}$ are the vehicle onboard accelerometers of x, y and z-axis compensated from the vehicle inclination. The vehicle heading change is estimated in equation 3.

$$\Delta\theta_{vehicle} = (VSR)\theta_{steering} \tag{3}$$

Where VSR is the Vehicle Steering Ratio which should be constant for each type and model of vehicles. $\Delta\theta_{vehicle}$ is the change of heading.

During GNSS signal availability, the reference navigation whether it is from GNSS only or GNSS/INS integrated system provides a reference heading change to model the errors (bias and scale factor) of the heading change estimated from CPD accelerometers as shown in Figure 3.

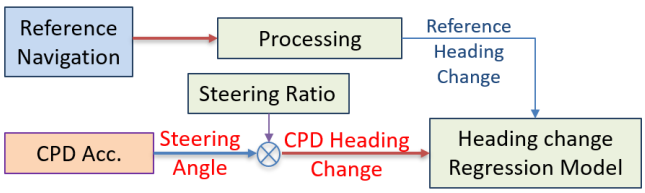

Figure 3. CPD Heading change errors modeling using the reference navigation system

2.2 DR navigation system based on CPD heading change and OBD-II velocity

The evaluated dead reckoning scheme is based on the estimated heading change by the CPD accelerometers and the vehicle forward velocity information obtained from a commercial On-Board Diagnosis II (OBD-II). Figure 4 depicts this DR navigation system.

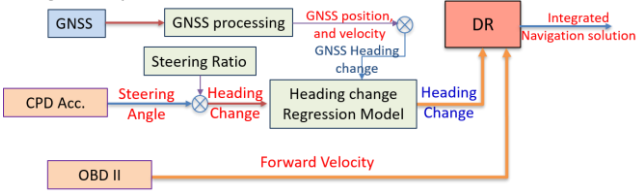

Figure 4. DR navigation system scheme based on CPD heading change and vehicle information

During GNSS signal availability, GNSS provides the land vehicle navigation solution in addition to the reference heading to calibrate the errors of the CPD heading change. On the other hand, During GNSS signal outages, the OBD-II forward velocity along with the change of heading estimated from the CPD forms a DR navigation system.
It is worth mentioning here that this proposed navigation solution doesn't require any on-board sensors as it is based only on the CPD mounted on the steering wheel and a commercial OBD-II which makes it a very low-cost navigation system.

2.3 DR navigation system based on CPD heading change, gyroscopes measurements and OBD-II velocity

This proposed navigation system is based on the vehicle information gathered from a commercial OBD-II and the heading change computed from the CPD accelerometer and a calibrated z-gyroscope from an on-board low-cost INS as shown in Figure 5.

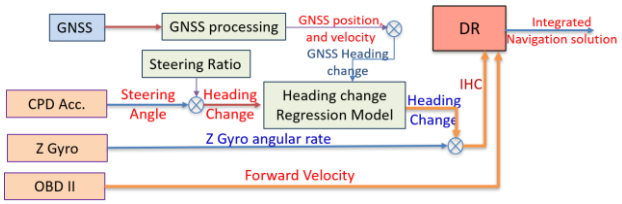

Figure 5. Proposed DR navigation system scheme based on CPD heading change, vehicle information, and onboard z-gyroscope.

An Integrated Heading Change (IHC) is computed using both the CPD heading change and the calibrated z-gyroscope angular rate. The DR system works during GNSS signal outage while the GNSS provides the navigation solution during its availability and calibrates the z-gyroscope as well the CPD heading change errors. The proposed navigation system is applied when there is an on-board INS, as well as a CPD, fixed on the steering wheel.

2.4 Typical 3D RISS navigation system

The main idea of the 3D RISS is described in (Noureldin, Aboelmagd, Karamat, Tashfeen and Georgy, 2013) and (Iqbal et al., 2008), it has been proposed to reduce some errors of the full inertial sensors system in addition to the reduction of the cost by using fewer sensors. 3D RISS systems consist of two accelerometers that are mounted in the forward and transverse moving directions in addition to a vehicle odometer as well as a vertical gyroscope which is mounted in the z-direction. The main function of the vertical gyroscope is to estimate the azimuth angle as shown in equation (4) and (5) (Noureldin, et al., 2013)

$$\dot{A} = -\left(\omega_z - \omega_e \sin\phi - \frac{v_e \tan\phi}{R_N + h}\right) \quad (4)$$

$$A_{k+1} = A_k - \left(\omega_z - \omega_e \sin\phi - \frac{v_e \tan\phi}{R_N + h}\right) dt \quad (5)$$

Where A is the azimuth angle, ω_z is the angular rotation rate in the z-direction measured by the vertical gyroscope, ω_e is the earth angular rotation, ϕ is the latitude, v_e is the velocity in the east direction, R_N is the prime vertical radius of curvature, h is the height and dt is the epoch time interval.
The rate of change of the azimuth angle is equal to the angular rotation measured by the vertical gyroscope considering two factors that should be compensated which are the earth rotation component in the z-direction and the change of the orientation of the Local Level Frame with respect to the Earth Fixed Frame (LLF w.r.t EFF) in the z-direction.
The main function of the odometer is to measure the velocity in the vehicle forward direction and thus the velocity in the east, north, and up directions can be determined as shown in the following equations (Noureldin, et al., 2013).

$$v_e = v_{od} \sin A \cos p \quad (6)$$

$$v_n = v_{od} \cos A \cos p \quad (7)$$

$$v_u = v_{od} \sin p \quad (8)$$

Where v_e, v_n, and v_u are the velocity in the east, north, and up directions respectively, while v_{od} is the velocity measured by the odometer and p is the pitch angle.
Finally, the function of the forward and the lateral accelerometers is to estimate the pitch (p) and the roll (r) angles. Originally, the forward accelerometer (f_y) measures the forward vehicle acceleration which can be calculated using the odometer as (a_{od}) as well as the gravity acceleration component in the forward direction and therefore the pitch angle can be calculated using equation (9).
On the other hand, the roll angle can be estimated through equation (10).

$$p = \sin^{-1}\left(\frac{f_y - a_{od}}{g}\right) \quad (9)$$

$$r = -\sin^{-1}\left(\frac{f_x + v_{od}\omega_z}{g \cos p}\right) \quad (10)$$

Where f_y and f_x are the specific forces measured by the forward and the lateral accelerometers respectively.
Finally, the position is calculated as follows:

$$\phi_{k+1} = \phi_k + \frac{v_n}{R_M + h} dt \quad (11)$$

$$\lambda_{k+1} = \lambda_k + \frac{v_e}{(R_N + h)\cos\phi} dt \quad (12)$$

$$h_{k+1} = h_k + v_u dt \quad (13)$$

where R_M is the meridian radius of curvature.
The typical 3D RISS integration scheme is depicted in Figure 6.

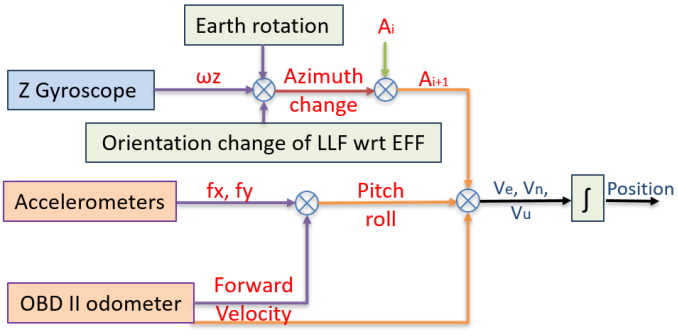

Figure 6. Typical 3D RISS navigation system scheme based on onboard sensors and vehicle information.

2.5 Modified 3D RISS navigation system

The proposed modified 3D RISS navigation system is based on OBD-II velocity, onboard gyroscopes, accelerometers, and CPD-based heading change as shown in Figure 7.

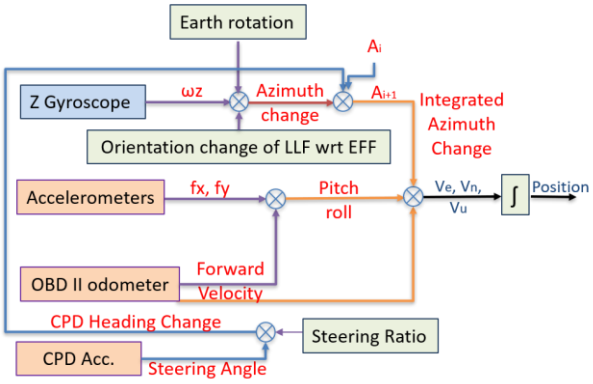

Figure 7. Modified 3D RISS navigation system scheme based on onboard sensors, CPD heading change, and vehicle information.

The CPD is mounted on the steering wheel to estimate the steering wheel angle and then the vehicle heading change is calculated. The Integrated Azimuth Change is calculated using a weighted mean between the CPD heading change and the z-gyroscope angular rate.

2.6 Loosely coupled GNSS/INS with different update types

Typical GNSS/INS loosely coupled integration scheme is based on GNSS that provides the navigation filter with position and velocity updates to aid the INS. During GNSS signal outages, INS should be aided to mitigate its large drift. Different update types are investigated which are: the forward velocity, the CPD-based change of heading, the z- gyroscope angular rate, the magnetometer heading, and Non-Holonomic Constraint (NHC) updates and different combinations between these updates.
Figure 8 shows the GNSS/INS integration scheme with vehicle forward velocity and CPD heading change updates.

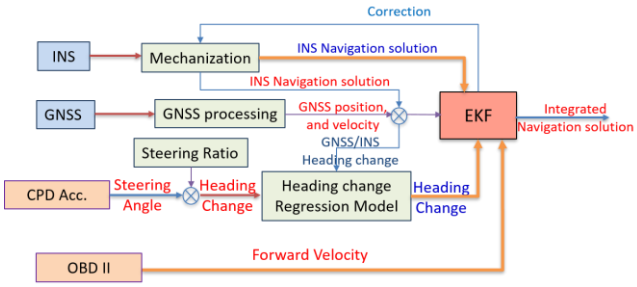

Figure 8. GNSS/INS loosely coupled navigation system scheme with updates based on CPD heading change and vehicle information

GNSS/INS loosely coupled integration is used to estimate the navigation solution through EKF during GNSS signal availability. While the proposed CPD heading change and the OBD-II forward velocity aids the low-cost INS during GNSS signal outage.
EKF is one of the most common navigation filters used in land vehicle navigation. It deals with the navigation states and the INS biases. The error states vector δx consists of 21 states as follows:

$$\delta x_{1\times 21} = \left[\delta P_{1\times 3} \quad \delta v_{1\times 3} \quad \delta \alpha_{1\times 3} \quad b_{a_{1\times 3}} \quad b_{g_{1\times 3}} \quad S_{a_{1\times 3}} \quad S_{g_{1\times 3}}\right]$$

where δP, δv, *and* $\delta \alpha$ are the position, the velocity, and the attitude error states respectively. b_a and b_g are the biases of the accelerometers and the gyroscopes respectively. Finally, S_a and S_g are the scale factor of the accelerometers and gyroscopes respectively.
There are two main stages of the KF- prediction and update stages. The system model describes the time evolution of the navigation states and is responsible for the prediction stage. On the other hand, the measurement model provides updates to the navigation filter. The KF models and stages equations are depicted in Figure 9.

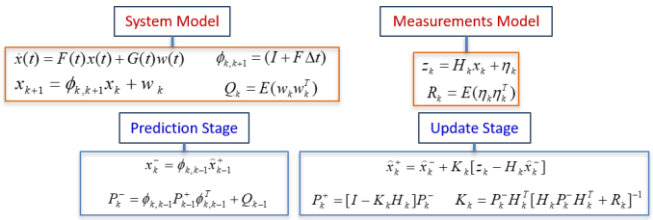

Figure 9. Kalman Filter system and measurement model along with the prediction and update stages.

Where $\dot{x}$ is the rate of change of the state vector, F is the dynamics matrix, x is the error state vector, G is the shaping matrix, and w_k is white noise. $\phi_{k,k+1}$ is the transition matrix, I is the identity matrix and Δt is the time interval, Q_k is the process noise matrix which defines the uncertainty of the system model. Finally, P_k is the states' covariance matrix. (-) refers to the predicted elements, and finally, (+) refers to updated elements, z_k is the observation vector, H_k is the design matrix, η_k is the measurement noise. R_k is the covariance matrix of the measurement noise which describes the uncertainty of the observations.

3. EXPERIMENTAL RESULTS

An experimental real data set was collected using Pixhawk 4 board which consists of a GNSS u-blox Neo-M8N receiver and ICM-20689 Invensense low-cost IMU in which its x-axis coincides with the forward vehicle direction. An iPhone 6 is used in the experiment which is mounted on the steering wheel of a Ford Focus car. A low-cost OBD-II interface (Uni-link Mini ELM327 OBD-II Bluetooth Scanner Tool) is used to access the regular odometer data from the vehicle.
The experiment was performed in an outdoor parking lot where different simulated GNSS signal outages were applied to the trajectory to show the impact of proposed techniques on the final navigation solution. Pixhawk 4 GNSS/INS integration is the reference navigation solution with sub-meter accuracy.
The experimental results are divided into two subsections which are the heading change regression model, and the heading change estimation results and different navigation systems results.

3.1 Heading Change Regression Model and Estimation Results

The steering wheel angle is estimated using CPD accelerometers where the CPD is attached to the steering wheel angle then the vehicle heading change is calculated using the estimated steering wheel angle. Linear regression is implemented to fit a model between the estimated heading change and the reference values. Figure 10 shows the regression

This contribution has been peer-reviewed. The double-blind peer-review was conducted on the basis of the full paper.
https://doi.org/10.5194/isprs-annals-V-1-2020-189-2020 | © Authors 2020. CC BY 4.0 License.

model between the steering wheel angle and the reference heading change.

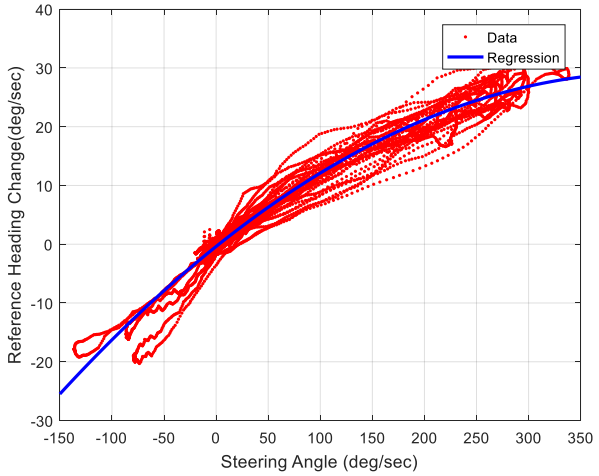

Figure 10. CPD regression model between the steering angle and the reference change of heading

The reference heading change is estimated either from the GNSS velocity or from GNSS/INS integration when using the typical loosely coupled integration scheme. Figure 11 exhibits the heading change estimated by the proposed method and the reference heading change.

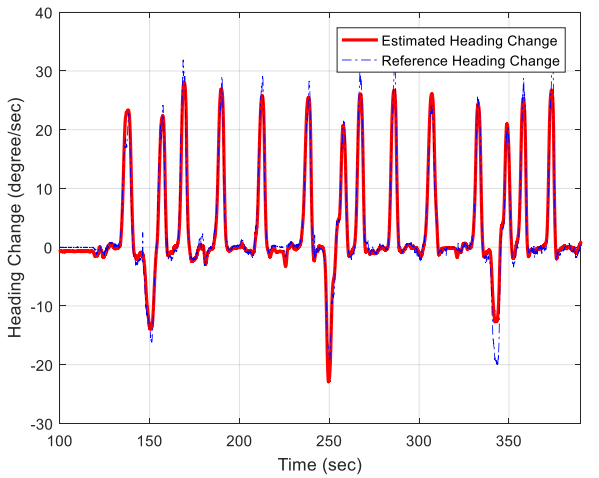

Figure 11. CPD change of heading versus the reference heading change

The difference between the change of heading estimated by the CPD accelerometers and the reference heading change is computed to assess the proposed method. The RMSE of the heading change estimation is 1.54 degrees/sec for around 290 seconds.

3.2 Navigation States Estimation Results

Navigation estimation results section is divided into three subsections which are: the dead reckoning results, the 3D RISS results, and results of loosely coupled INS integration with different updates. The vehicle trajectory consists of three loops where the outages are chosen for the second and/or third loop.

3.2.1 DR based on CPD heading change and OBD-II velocity results

DR navigation system is based on the land vehicle heading change estimated from the CPD accelerometers that are mounted on the vehicle steering wheel. The velocity information is obtained from the regular odometer from OBD-II. Figures 12 and 13 show the DR trajectory along with the reference for two GNSS outage periods of 90 seconds and 180 seconds respectively.

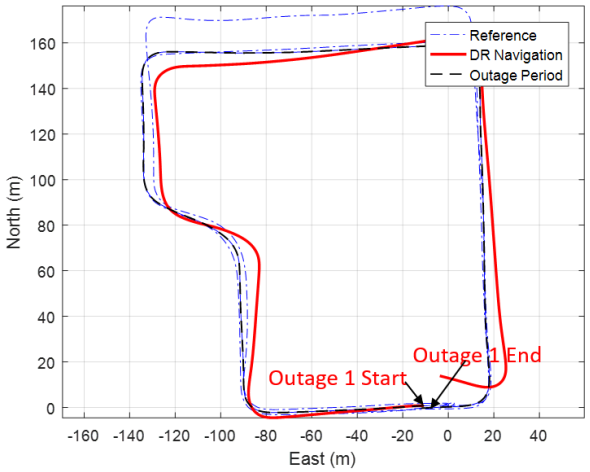

Figure 12. DR trajectory for 90 seconds GNSS signal outage

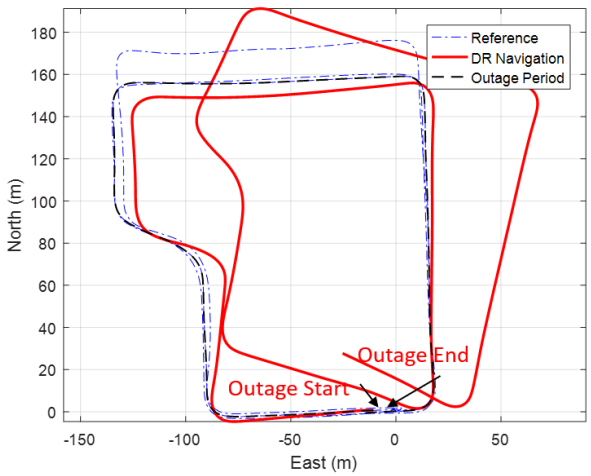

Figure 13. DR trajectory for 180 seconds GNSS signal outage

The DR trajectory is close to the reference trajectory during the 90 seconds outage period while it deviates at the beginning of the second 90 seconds. Table 1 shows the position RMSE foe DR system for different GNSS signal outages.

Navigation solution	RMSE (m)
Outage 1 (90 seconds)	7.63
Outage 2 (90 seconds)	12.88
Outage (180 seconds)	32.58

Table 1. Position RMSE for DR navigation solution method for different GNSS signal outage

3.2.2 DR based on CPD heading change, gyroscopes measurements and OBD-II velocity Results

This proposed navigation system depends on the CPD accelerometers as well as the on-board IMU gyroscope for providing heading change information to the system while the OBD-II provides the vehicle forward velocity. Figure 14, and 15 depicts the DR trajectory with the reference and the outage period.

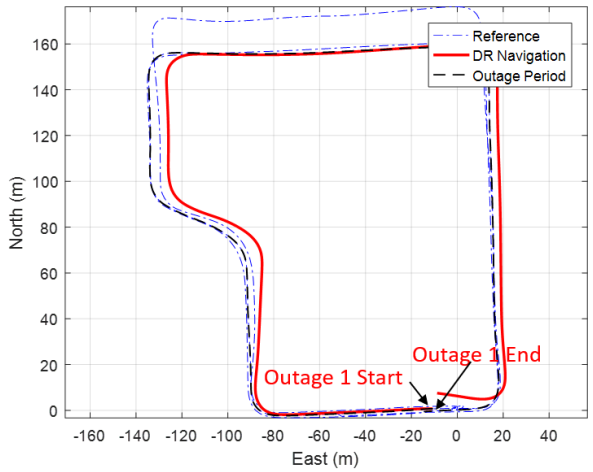

Figure 14. DR trajectory based on CPD sensors and onboard gyroscope for 90 seconds GNSS signal outage

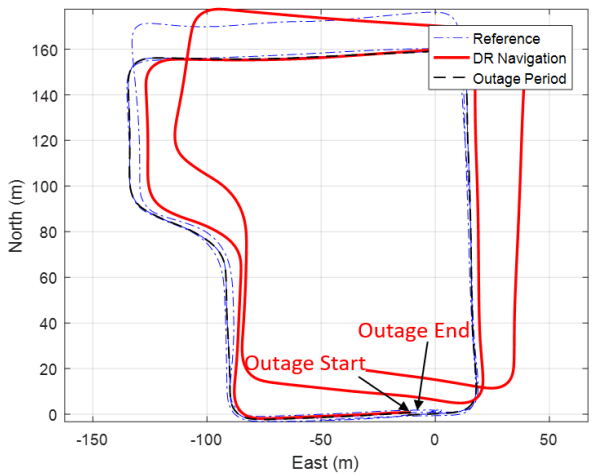

Figure 15. DR trajectory based on CPD sensors and onboard gyroscope for 180 seconds GNSS signal outage

If the system depends only on the gyroscope in providing the heading change information along with the OBD-II velocity, the position RMSE is around 7.80 meters for 90 seconds GNSS signal outage. However, integrating the heading change information from both the CPD sensors and onboard gyroscopes provides a better position estimation. Table 2 shows the position RMSE for this navigation system for different GNSS signal outages.

Navigation solution	RMSE (m)
Outage 1 (90 seconds)	6.03
Outage 2 (90 seconds)	6.97
Outage (180 seconds)	18.68

Table 2. Position RMSE for DR navigation solution method based on both CPD heading change and gyroscope for different GNSS signal outage

3.2.3 Typical 3D RISS Navigation Results

Typical 3D RISS navigation system is based on the compensated on-board z gyroscope, the x and y accelerometers and the forward velocity from a regular odometer. Figures 16 and 17 show the typical 3D RISS trajectory along with the reference trajectory and the GNSS outage period for 90 seconds and 180 seconds GNSS signal outages respectively.

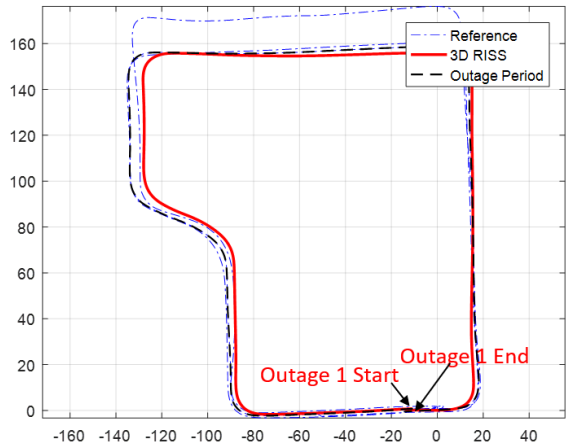

Figure 16. Typical 3D RISS trajectory for 90 seconds GNSS signal outage

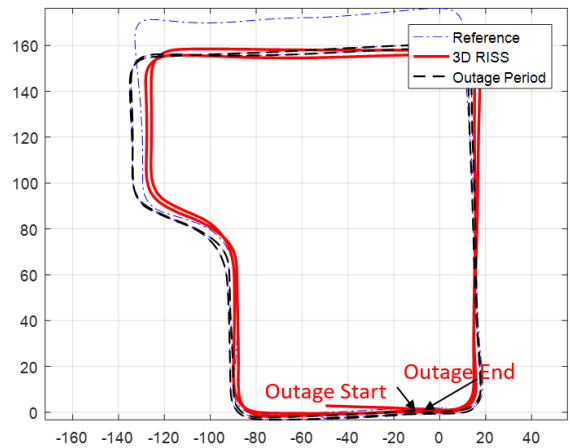

Figure 17. Typical 3D RISS trajectory for 180 seconds GNSS signal outage

Table 3 shows the position RMSE for different GNSS signal outages for typical 3D RISS navigation system.

Navigation solution	RMSE (m)
Outage 1 (90 seconds)	5.06
Outage 2 (90 seconds)	4.90
Outage (180 seconds)	6.12

Table 3. Position RMSE for 3D RISS navigation solution method for different GNSS signal outage

The navigation state estimation is improved where the average position RMSE is around 5.00 meters for 90 seconds GNSS signal outage.

3.2.4 Modified 3D RISS Navigation Results

Modified 3D RISS depends on the compensated on-board z gyroscope along with the CPD mounted on the steering wheel for providing the land vehicle heading change. Figure 18 and 19 exhibits the modified 3D RISS, reference trajectory and the outage period.

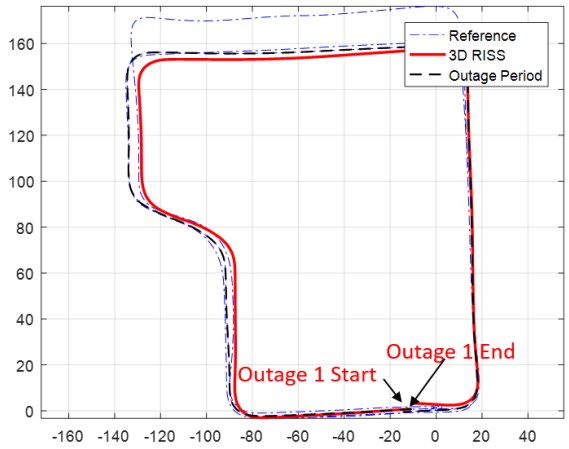

Figure 18. Modified 3D RISS trajectory for 90 seconds GNSS signal outage

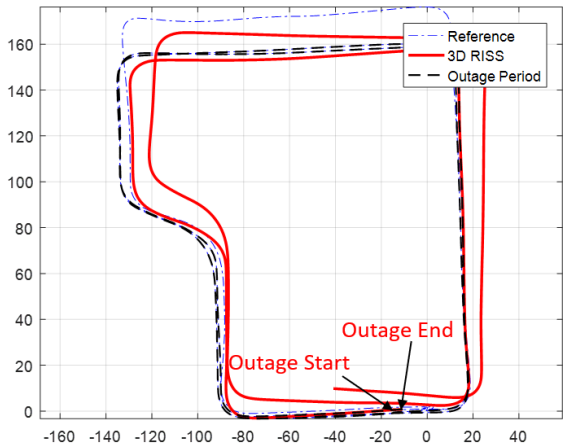

Figure 19. Modified 3D RISS trajectory for 180 seconds GNSS signal outage

Table 4 shows the position RMSE of the modified 3D RISS for different GNSS signal outages.

Navigation solution	RMSE (m)
Outage 1 (90 seconds)	4.37
Outage 2 (90 seconds)	3.46
Outage (180 seconds)	9.90

Table 4. Position RMSE for modified 3D RISS with steering angle navigation solution method for different GNSS signal outage

Modified 3D RISS provides a better navigation state estimation for 90 seconds GNSS signal outage with 3.9 meters average position RMSE. However, the position accuracy deteriorates for 180 seconds GNSS signal outage because of the CPD heading change drift at the beginning of the second 90 seconds outage.

3.2.5 Typical INS with different updates Navigation Results

Loosely coupled GNSS/INS integration is implemented for the navigation state estimation. Figures 20 and 21 show the land vehicle trajectory in case of INS standalone solution for 90 seconds and 180 seconds GNSS signal outage respectively.
Table 5 shows the position RMSE for different GNSS signal outages for uncalibrated INS standalone navigation system.

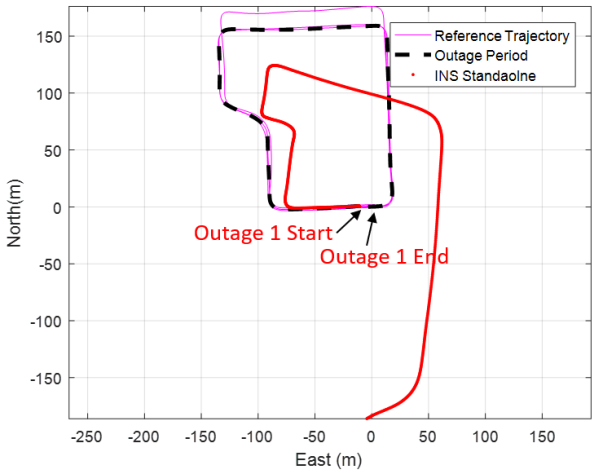

Figure 20. INS standalone trajectory for 90 seconds GNSS signal outage

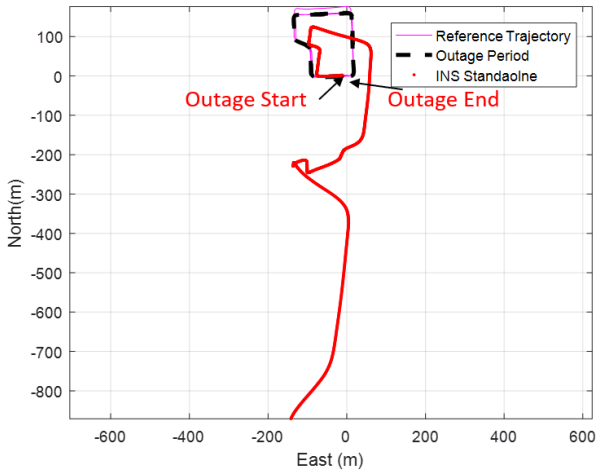

Figure 21. INS standalone trajectory for 180 seconds GNSS signal outage

Navigation solution	RMSE (m)
Outage 1 (90 seconds)	90.15
Outage 2 (90 seconds)	60.20
Outage (180 seconds)	352.59

Table 5. Position RMSE for INS standalone navigation solution method for different GNSS signal outage

The INS standalone navigation solution deteriorates due to the low-cost IMU large drift because of the errors of both accelerometers and gyroscopes. INS should be aided during GNSS signal outage to limit its drift.
Different updates are implemented to aid the INS such as the CPD heading change, OBD-II velocity, z gyroscope angular rate, and NHC. Tables 6 and 7 show position RMSE for different update types for 90s and 180s GNSS signal outages respectively. Figure 22 shows different types of updates with INS trajectories for 90 seconds of GNSS signal outage.

Navigation solution	RMSE (m)
INS standalone	90.15
INS/OBD-II velocity	5.82
INS/NHC	4.66
INS/velocity/NHC/CPD heading change	3.17
INS/velocity/NHC/gyro angular rate	3.26
INS/velocity/NHC/IHR	3.20

Table 6. Position RMSE for INS/different updates navigation solution method for 90 seconds GNSS signal outage

This contribution has been peer-reviewed. The double-blind peer-review was conducted on the basis of the full paper.
https://doi.org/10.5194/isprs-annals-V-1-2020-189-2020 | © Authors 2020. CC BY 4.0 License.

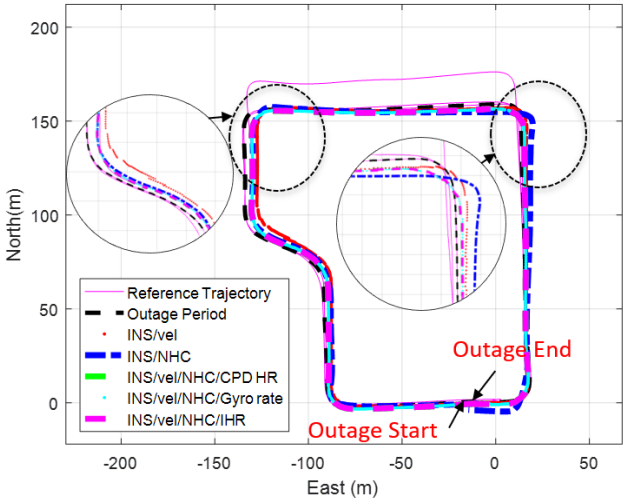

Figure 22. INS/different updates trajectory for 90 seconds GNSS signal outage

Navigation solution	RMSE (m)
INS standalone	352.59
INS/OBD-II velocity	18.28
INS/NHC	11.77
INS/velocity/NHC/CPD heading change	5.98
INS/velocity/NHC/gyro angular rate	6.05
INS/velocity/NHC/IHR	6.00

Table 7. Position RMSE for navigation solution of INS/different updates for 180 seconds GNSS signal outage

Aiding low-cost INS with OBD II velocity, NHC, and CPD heading change provides the best navigation state estimation where the RMSE of the position is around 3.1 and 6 meters for 90s and 180s GNSS signal outage respectively.

4. CONCLUSIONS

Different land vehicle navigation systems were implemented and investigated using CPD sensors, onboard sensors, and vehicle information. The navigation systems are based on different DR, RISS, and typical GNSS/INS integration systems with different updates. These navigation systems could be implemented in a GNSS denied environment such as in urban canyons, foliage areas, tunnels, and underground parking. Typical RISS shows better navigation results than the DR systems for 90s and 180s GNSS signal outage while modified RISS provides a better navigation solution than the typical RISS system. Finally, CPD heading change/OBD-II velocity/NHC integrated aiding system with INS provides the best navigation state estimation for various GNSS signal outages.

ACKNOWLEDGMENTS

This work was supported by Dr. Naser El-Sheimy research funds from NSERC and Canada Research Chairs programs.

REFERENCES

Abd Rabbou, M., El-Rabbany, A., 2015. Integration of GPS precise point positioning and MEMS-based INS using unscented particle filter. Sensors (Switzerland) 15, 7228–7245. https://doi.org/10.3390/s150407228

Abosekeen, A., Noureldin, A., Korenberg, M.J., 2019. Improving the RISS / GNSS Land-Vehicles Magnetic Azimuth Updates. IEEE Trans. Intell. Transp. Syst. PP, 1–14. https://doi.org/10.1109/TITS.2019.2905871

Aggarwal, P., Syed, Z., El-Sheimy, N., 2008. Thermal calibration of low cost MEMS sensors for land vehicle navigation system. IEEE Veh. Technol. Conf. 2859–2863. https://doi.org/10.1109/VETECS.2008.623

Attia, M., 2013. Map Aided Indoor and Outdoor Navigation Applications. University of Calgary.

Bancroft, J.B., 2009. Multiple IMU Integration for Vehicular Navigation. Proc. ION GNSS 2009 22–25.

Bo, Y., Yue-gang, W., Liang, X., Bin, S., Bao-cheng, W., 2018. Accurate integrated position and orientation method for vehicles based on strapdown inertial navigation system / Doppler radar. Meas. Control 51, 431–442. https://doi.org/10.1177/0020294018792349

Gao, Y., Liu, S., Atia, M.M., Noureldin, A., 2015. INS/GPS/LiDAR integrated navigation system for urban and indoor environments using hybrid scan matching algorithm. Sensors (Switzerland) 15, 23286–23302. https://doi.org/10.3390/s150923286

Georgy, J., Member, Student, Noureldin, A., Member, Senior, Korenberg, M.J., Bayoumi, M.M., 2010a. Low-Cost Three-Dimensional Navigation Solution for RISS / GPS Integration Using Mixture Particle Filter. IEEE Trans. Veh. Technol. 59, 599–615. https://doi.org/10.1109/TVT.2009.2034267

Georgy, J., Noureldin, A., Syed, Z., Goodall, C., 2010b. Nonlinear Filtering for Tightly Coupled RISS / GPS Integration. IEEE/ION Position, Locat. Navig. Symp. 1014–1021. https://doi.org/10.1109/PLANS.2010.5507327

Iqbal, U., Georgy, J., Korenberg, M.J., Noureldin, A., 2010. Augmenting Kalman filtering with parallel cascade identification for improved 2D land vehicle navigation. IEEE Veh. Technol. Conf. https://doi.org/10.1109/VETECF.2010.5594107

Iqbal, U., Okou, A.F., Noureldin, A., 2008. An Integrated Reduced Inertial Sensor System - RISS / GPS for Land Vehicle 1014–1021.

Liu, Zhenbo, El-Sheimy, Naser, Yu , Chunyang, Qin, Y., 2018. Motion Constraints and Vanishing Point Aided Land Vehicle Navigation. micromachines 9, 1–24. https://doi.org/10.3390/mi9050249

Moussa, M, Moussa, A., El-sheimy, N., 2019. Ultrasonic Wheel Based Aiding for Land Vehicle Navigation in GNSS denied environment, in: Proceedings of the 2019 International Technical Meeting, ION ITM 2019, Reston, Virginia,. pp. 319–333.

Moussa, Mohamed, Moussa, A., El-Sheimy, N., 2019. Steering Angle Assisted Vehicular Navigation Using Portable Devices in GNSS-Denied Environments. Sensors 19, 1618. https://doi.org/10.3390/s19071618

Moussa, M., Moussa, A., El-Sheimy, N., 2018. Ultrasonic based heading estimation for aiding land vehilce navigation in GNSS denied environment. ISPRS TC I Mid-term Symp. Innov. Sens. – From Sensors to Methods Appl. XLII, 10–12.

Niu, X., Nassar, S., El-Sheimy, N., 2007. An Accurate Land-Vehicle MEMS IMU/GPS Navigation System Using 3D Auxiliary Velocity Updates. J. Inst. Navig. 54, 177–188.

Noureldin, Aboelmagd, Karamat, Tashfeen and Georgy, J., 2013. Fundamentals of Inertial Navigation Satellite-based Positioning and their integration. Springer-Verlag Berlin Heidelberg 2013.

Sathe, A.D., Deshmukh, V.D., 2017. Advance vehicle-road interaction and vehicle monitoring system using smart phone applications. Proc. 2016 Online Int. Conf. Green Eng. Technol. IC-GET 2016. https://doi.org/10.1109/GET.2016.7916825

Song, T., Capurso, N., Cheng, X., Yu, J., Chen, B., Zhao, W., 2017. Enhancing GPS with Lane-Level Navigation to Facilitate Highway Driving. IEEE Trans. Veh. Technol. 66, 4579–4591. https://doi.org/10.1109/TVT.2017.2661316

Tang, J., Chen, Y., Niu, X., Wang, L., Chen, L., Liu, J., Shi, C., Hyyppa, J., 2015. LiDAR scan matching aided inertial navigation system in GNSS-denied environments. Sensors (Switzerland) 15, 16710–16728. https://doi.org/10.3390/s150716710

Venkatraman, K., Karthick, Amutha, B., Sankar, S.R., 2010. A hybrid method for improving GPS accuracy for land vehicle navigation system. Int. Conf. "Emerging Trends Robot. Commun. Technol. INTERACT-2010 74–79. https://doi.org/10.1109/INTERACT.2010.5706204

Wahlström, J., Skog, I., Händel, P., 2017. Smartphone-Based Vehicle Telematics: A Ten-Year Anniversary. IEEE Trans. Intell. Transp. Syst. 18, 2802–2825. https://doi.org/10.1109/TITS.2017.2680468

Won, D., Ahn, J., Sung, S., Heo, M., Im, S.H., Lee, Y.J., 2015. Performance Improvement of Inertial Navigation System by Using Magnetometer with Vehicle Dynamic Constraints. J. Sensors 2015. https://doi.org/10.1155/2015/435062

Xiao, Z., Li, P., Havyarimana, V., Georges, H.M., Wang, D., Li, K., 2018. GOI : A Novel Design for Vehicle Positioning and Trajectory Prediction Under Urban Environments. IEEE Sens. J. 18, 5586–5594. https://doi.org/10.1109/JSEN.2018.2826000

Zhenbo Liu, 2019. Vision Sensor Aided Navigation for Ground Vehicle Applications. University of Calgary.

Zhu, S., Wang, Xiong, Zhang, Z., Tian, X., Wang, Xinbing, 2017. Lane-level vehicular localization utilizing smartphones. IEEE Veh. Technol. Conf. https://doi.org/10.1109/VTCFall.2016.7881065